Journal of Hazardous Materials 180 (2010) 741–747

Contents lists available at ScienceDirect

Journal of Hazardous Materials

journal homepage: www.elsevier.com/locate/jhazmat

Toxic interaction mechanism between oxytetracycline and bovine hemoglobin

Zhenxing Chi, Rutao Liu*, Bingjun Yang, Hao Zhang

School of Environmental Science and Engineering, Shandong University, China-America CRC for Environment & Health, 27# Shanda South Road, Jinan, Shandong Province 250100, PR China

ARTICLE INFO

Article history:
Received 4 March 2010
Received in revised form 25 April 2010
Accepted 26 April 2010
Available online 4 May 2010

Keywords:
Oxytetracycline
Bovine hemoglobin
Fluorescence quenching
UV–vis spectroscopy
CD spectroscopy
Molecular modeling

ABSTRACT

Oxytetracycline (OTC) is a kind of widely used veterinary drugs. The residue of OTC in the environment is potentially harmful. In the present work, the interaction between OTC and bovine hemoglobin (BHb) was investigated by fluorescence, synchronous fluorescence, UV–vis absorption, circular dichroism and molecular modeling techniques under physiological conditions. The experimental results showed that OTC can bind with BHb to form complex. The binding process is a spontaneous molecular interaction procedure, in which van der Waals and hydrogen bonds interaction play a major role. The number of binding sites were calculated to be 1.12 (296 K), 1.07 (301 K) and 0.95 (308 K), and the binding constants were of $K_{296\,K} = 9.43 \times 10^4\,L\,mol^{-1}$, $K_{301\,K} = 4.56 \times 10^4\,L\,mol^{-1}$ and $K_{308\,K} = 1.12 \times 10^4\,L\,mol^{-1}$ at three different temperatures. Based on the Förster theory of nonradiative energy transfer, the binding distance between OTC and the inner tryptophan residues of BHb was determined to be 2.37 nm. The results of UV–vis absorption, synchronous fluorescence and CD spectra indicated that OTC can lead to conformational and some microenvironmental changes of BHb, which may affect physiological functions of hemoglobin. The synchronous fluorescence experiment revealed that OTC binds into hemoglobin central cavity, which was verified by molecular modeling study. The work is helpful for clarifying the molecular toxic mechanism of OTC in vivo.

1. Introduction

The annual output of antibiotics in china was estimated to be about 210,000 tons in 2005, and about 90,000 tons are used as animal feed additives or for therapeutic purposes [1]. Tetracyclines are one of the most extensively used antibiotics in animal feeding operations. Similar to other antibiotics, they are excreted mostly as the parent compound, representing 50–80% of the applied dose [2]. Oxytetracycline (OTC) is a broad-spectrum bacteriostatic antibiotic that belongs to the tetracycline antibiotics [3,4]. It has been widely used as feed additive for therapy of systemic bacterial infections in farmed fish, as a growth stimulator in livestock and as prophylactic treatment of bacterial diseases in plants [4]. The Joint FAO/WHO Expert Committee of Food Additives and Contaminants (JECFA), at its 50th Meeting in 1998, established a group acceptable daily intake (ADI) of 0–0.03 mg kg^{-1} body weight for the tetracyclines (oxytetracycline (OTC), tetracycline (TC) and chlortetracycline (CTC)), alone or in combination. The committee also recommended maximum residue limits (MRLs) of 100 μg L^{-1} in milk and muscle of all food-producing species [5,6]. OTC can enter the environment via wastewater effluent discharges, agricultural runoff et al., being detected at nanogram to low-microgram per liter levels in wastewater effluents and natural waters [7]. When OTC enter the organism, it can inhibit the antibody levels in fish [8], induce DNA damage in carp kidney cells [9], interact with cytoplasmic protein synthesis [10] and induce blood disorder in Juvenile Nile Tilapia *Oreochromis niloticus* [11].

Hemoglobin (Hb) is a protein responsible for oxygen carrying in the vascular system of animals. It can also aid the transport of carbon dioxide, regulate the pH of blood and remove hydrogen ions in the capillaries and carries them to the lungs [12]. Except for albumin, as a kind of intracellular protein, hemoglobin can also function as binders of drugs [13]. When the residue of the veterinary drugs in the environment enter organism, they may penetrate erythrocytes and interact with Hb [13]. OTC can significantly reduce the erythrocyte count and Hb value [11]. However, the interaction mechanism between OTC and bovine hemoglobin has not been reported.

In the present work, we studied in vitro interaction of OTC with bovine hemoglobin (BHb) under the simulative physiological conditions by using fluorescence quenching, UV absorption spectrometry, synchronous fluorescence, circular dichroism and molecular modeling techniques. The binding mechanism of OTC with BHb (association constants, thermodynamic parameters, the number of binding sites, the binding forces, the specific binding site, and the energy transfer distance between OTC and BHb) was estimated. The effect of OTC on BHb conformation was also discussed.

* Corresponding author. Tel.: +86 531 88364868; fax: +86 531 88364868.
E-mail address: rutaoliu@sdu.edu.cn (R. Liu).

0304-3894/$ – see front matter © 2010 Elsevier B.V. All rights reserved.
doi:10.1016/j.jhazmat.2010.04.110

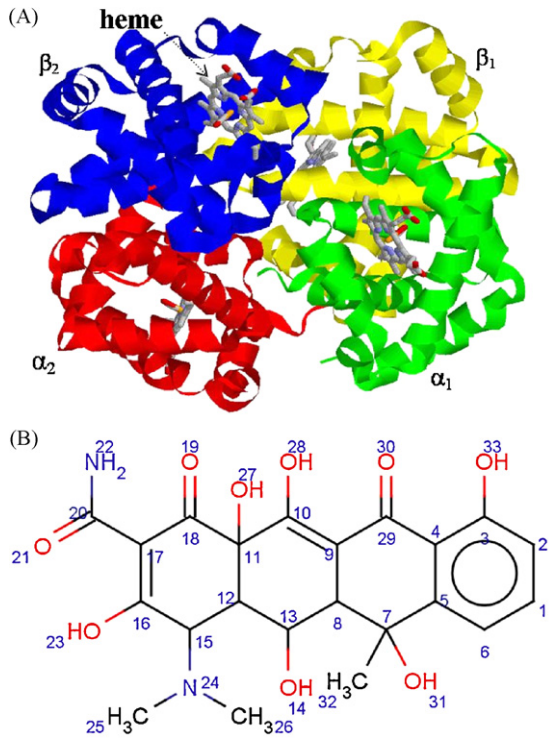

Fig. 1. (A) Molecular structure of BHb (PDB code 1G09) and (B) molecular structure of OTC with with atom numbers.

The study can provide the basic data for understanding the toxicity mechanism of OTC in vivo.

2. Materials and methods

2.1. Reagents

BHb (Beijing Biodee Biotechnology, Co., Ltd.) was dissolved in ultrapure water to form 3.0×10^{-5} mol L^{-1} solution, then preserved at 0–4 °C and diluted as required. The molecular structure of BHb (PDB code 1G09) is shown in Fig. 1(A) [14].

A stock solution of OTC (1.0×10^{-3} mol L^{-1}) was prepared by dissolving 0.0461 g OTC (Beijing Shanglifang Joint Chemical Technology Research Institute) in 100 mL of water. Hydrochloric acid solution (1:1) was used to promote dissolution. The molecular structure of OTC is shown in Fig. 1(B).

A 0.2 mol L^{-1} of phosphate buffer (mixture of $NaH_2PO_4{\cdot}2H_2O$ and $Na_2HPO_4{\cdot}12H_2O$, pH 7.4) was used to control pH. $NaH_2PO_4{\cdot}2H_2O$ and $Na_2HPO_4{\cdot}12H_2O$ were of analytical reagent grade, obtained from Tianjin Damao Chemical Reagent Factory.

2.2. Apparatus and methods

All fluorescence spectra were recorded on an F-4600 Spectrofluorimeter (Hitachi, Japan). The excitation and emission slit widths were set at 5.0 nm. The scan speed was 1200 nm/min. PMT (Photo Multiplier Tube) voltage was 700 V.

The UV–vis absorption spectra were measured on a UV-2450 spectrophotometer (SHIMADZU, Kyoto, Japan). CD spectra were recorded on a J-810 circular dichroism spectrometer (JASCO). The pH measurements were made with a pHs-3C acidity meter (Pengshun, Shanghai, China).

2.3. Experimental procedures

The fluorescence measurements were carried out as follows: to each of a series of 10 mL test-tube, 1.0 mL of 0.2 mol L^{-1} phosphate buffer (pH 7.4) and 1.0 mL of 3.0×10^{-5} mol L^{-1} BHb were added, followed by different amounts of 1.00×10^{-3} mol L^{-1} stock solution of OTC. The fluorescence spectra were then measured (excitation at 280 nm and emission wavelengths range 290–420 nm). The synchronous fluorescence spectra were obtained through simultaneous scanning of the excitation (λ_{ex} = 250 nm) and emission monochromators while maintaining a constant wavelength interval between them ($\Delta\lambda$, 15 nm and 60 nm). CD spectra were collected from 200 to 260 nm with three scans averaged for each CD spectrum.

In order to eliminate the inner filter effects of protein and ligand, absorbance measurements were performed at excitation and emission wavelengths of the fluorescence measurements. The fluorescence intensity was corrected using the equation [15]:

$$F_{cor} = F_{obs} 10^{(A_1+A_2)/2} \quad (1)$$

where F_{cor} and F_{obs} are the fluorescence intensity corrected and observed, respectively; A_1 and A_2 are the sum of the absorbances of protein and ligand at excitation and emission wavelengths, respectively.

2.4. Molecular modeling study

Docking calculations were carried out using DockingServer. The MMFF94 force field [16] was used for energy minimization of ligand molecule (OTC) using DockingServer. PM6 semiempirical charges calculated by MOPAC2009 [17] were added to the ligand atoms. Nonpolar hydrogen atoms were merged, and rotatable bonds were defined.

Docking calculations were carried out on BHb protein model. Essential hydrogen atoms, Kollman united atom type charges, and solvation parameters were added with the aid of AutoDock tools [18]. Affinity (grid) maps of 100 Å × 100 Å × 100 Å grid points and 0.375 Å spacing were generated using the Autogrid program [18]. AutoDock parameter set- and distance-dependent dielectric functions were used in the calculation of the van der Waals and the electrostatic terms, respectively.

Docking simulations were performed using the Lamarckian genetic algorithm (LGA) and the Solis and Wets local search method [19]. Initial position, orientation, and torsions of the ligand molecules were set randomly. Each run of the docking experiment was set to terminate after a maximum of 250,000 energy evaluations. The population size was set to 150. During the search, a translational step of 0.2 Å, and quaternion and torsion steps of 5 were applied.

3. Results and discussion

3.1. Fluorescence quenching of BHb by OTC

The fluorescence technique can be used to investigate the binding information of small molecules to protein such as the binding mechanism, binding mode, binding constants and intermolecular distances. We utilized the technique to study the interaction between BHb and OTC.

BHb contains three Trp and five Tyr residues in each αβ dimer, for a total of six Trp and ten Tyr residues in the tetramer [20]. Though all the Trp and Tyr residues contribute to the intrinsic fluorescence of BHb, it primarily originates from β-37 Trp that plays a key role in the quaternary state change upon ligand binding [21]. Changes in the intrinsic fluorescence of BHb can provide considerable information about its structure and dynamics [20].

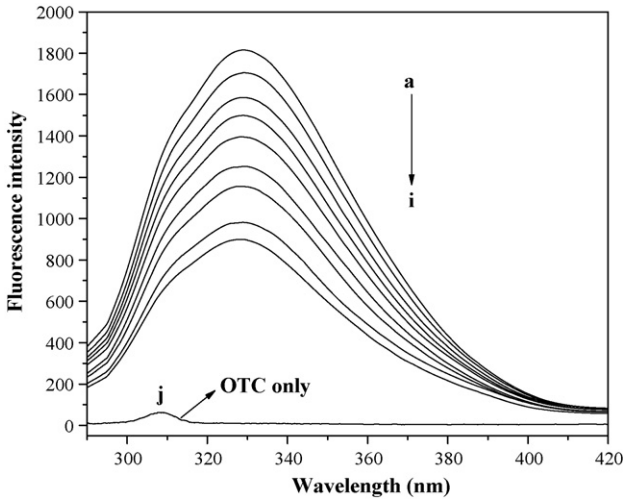

Fig. 2. Effect of OTC on BHb fluorescence (corrected). Conditions: BHb: 3×10^{-6} mol L^{-1}; OTC/(10^{-5} mol L^{-1}): (a) 0, (b) 0.4, (c) 0.8, (d) 1.2, (e) 1.6, (f) 2, (g) 2.8, (h) 3.6, (i) 4 and (j) OTC only, 4×10^{-5} mol L^{-1}, pH 7.4 and T = 301 K.

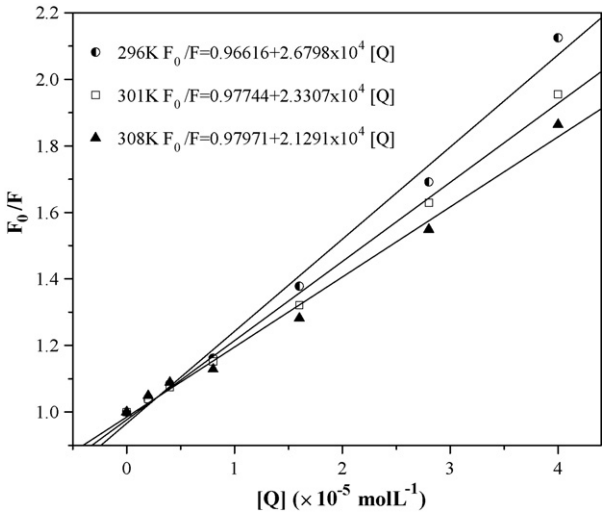

Fig. 3. Stern–Volmer plots for the quenching of BHb by OTC at different temperatures (corrected). Conditions: BHb: 3×10^{-6} mol L^{-1}; pH 7.4.

Table 1
Stern–Volmer quenching constants for the interaction of OTC with BHb at three different temperatures.

pH	T (K)	K_{SV} ($\times 10^5$ L mol^{-1})	k_q ($\times 10^{12}$ L mol^{-1} s^{-1})	R[a]	S.D.[b]
7.4	296	0.26798	2.6798	0.99459	0.04056
	301	0.23307	2.3307	0.99451	0.03555
	308	0.21291	2.1291	0.99282	0.03717

[a] R is the correlation coefficient.
[b] S.D. is the standard deviation for the K_{SV} values.

The effect of OTC on BHb fluorescence intensity is shown in Fig. 2. It can be seen that the fluorescence of BHb can be quenched by OTC. Quenching mechanisms include static and dynamic quenching. In order to confirm the quenching mechanism, the fluorescence quenching data were analyzed according to the Stern–Volmer equation [22]:

$$\frac{F_0}{F} = 1 + K_{sv}[Q] = 1 + k_q \tau_0 [Q] \quad (2)$$

where F_0 and F are the fluorescence intensities in the absence and presence of the quencher, respectively. K_{SV}, [Q], k_q and τ_0 are the Stern–Volmer quenching constant, the concentration of the quencher, the quenching rate constant of the biological macromolecule and the fluorescence lifetime in the absence of quencher, respectively. The Stern–Volmer plot before correction was non-straight, so the Stern–Volmer equation cannot be used to calculate the K_{SV} and k_q. After corrected with Eq. (1), the plot agrees well with the Stern–Volmer Eq. (2). The corrected Stern–Volmer plots for the quenching of BHb by OTC at three different temperatures are shown in Fig. 3. The calculated K_{SV} and k_q values at three different temperatures were listed in Table 1.

Quenching type should be single static or dynamic quenching. Since higher temperature results in larger diffusion coefficients, the dynamic quenching constants will increase with increasing temperature. In contrast, increased temperature is likely to result in decreased stability of complexes, and thus the static quenching constants are expected to decrease with increasing temperature [23]. In addition, the maximum scatter collision quenching constant of various quenchers with the biopolymer was 2.0×10^{10} L mol^{-1} s^{-1} [24]. In this paper, the K_{SV} values decreased with increasing temperature and the k_q was greater than 2.0×10^{10} L mol^{-1} s^{-1}. This indicates that the quenching was not initiated from dynamic collision but from the formation of a complex.

3.2. The association constants and the number of binding sites

For the static quenching interaction, when small molecules bind independently to a set of equivalent sites on a macromolecule, the binding constant (K_a) and the number of binding sites (n) can be determined by the following equation [25]:

$$lg\frac{(F_0 - F)}{F} = lg\ K_a + n\, lg[Q] \quad (3)$$

where F_0, F and [Q] are the same as in Eq. (2), K_a is the binding constant and n is the number of binding sites per BHb molecule. According to Eq. (3), values of n and K_a (shown in Table 2) at physiological pH 7.4 were calculated. The number of binding sites n approximately equals to 1, indicating that there is one binding site in BHb for OTC. The value of K_a obtained is of the order of 10^4, indicating that there is a strong interaction between OTC and BHb. Even low concentrations of OTC in the blood can interact with BHb easily.

3.3. Thermodynamic parameters and binding forces

The acting forces between small organic molecules and biomolecules include hydrogen bonds, van der Waals interactions, electrostatic forces and hydrophobic interaction forces. If the temperature changes little, the reaction enthalpy change (ΔH°) is

Table 2
Binding constants and relative thermodynamic parameters of the OTC–BHb system.

T (K)	K_a ($\times 10^4$ L mol^{-1})	n	R[a]	ΔH° (kJ mol^{-1})	ΔS° (J mol^{-1} K^{-1})	ΔG° (kJ mol^{-1})
296	9.4256	1.12478	0.99926		−347.81	−28.187
301	4.5617	1.06936	0.99904	−131.14	−346.49	−26.847
308	1.1187	0.94929	0.99158		−348.27	−23.872

[a] R is the correlation coefficient for the K_a values.

regarded as a constant. The interaction parameters can be calculated on the basis of the van't Hoff equation and thermodynamic equation:

$$\ln\left(\frac{(K_a)_2}{(K_a)_1}\right) = \left(\frac{1}{T_1} - \frac{1}{T_2}\right)\left(\frac{\Delta H^\circ}{R}\right) \quad (4)$$

$$\Delta G^\circ = \Delta H^\circ - T\Delta S^\circ = -RT \ \ln K_a \quad (5)$$

where $(K_a)_1$ and $(K_a)_2$ are the binding constants at T_1 and T_2, R is the universal gas constant. ΔG° and ΔS° are the free-energy change and the entropy change of the binding reaction, respectively.

If $\Delta H < 0$ and $\Delta S < 0$, van der Waals' interactions and hydrogen bonds play a major role in the binding reaction. If $\Delta H > 0$ and $\Delta S > 0$, hydrophobic interactions are dominant. Electrostatic forces are more important when $\Delta H < 0$ and $\Delta S > 0$ [26]. The calculated thermodynamic parameters and K_a values for the binding interaction between OTC and BHb are listed in Table 2. The negative ΔH° and negative ΔS° indicated that van der Waals interactions and hydrogen bonds play the major role during the interaction. The negative sign of ΔG° indicates the spontaneity of the binding process of OTC with BHb [20].

3.4. Energy transfer between OTC and BHb

According to Förster's dipole–dipole nonradiative energy transfer theory [27], energy transfer from one molecular (donor) to another molecular (acceptor) will happen under the following conditions: (a) the energy donor can produce fluorescence; (b) the absorption spectrum of the receptor overlaps enough with the donor's fluorescence emission spectrum; (c) the distance between the donor and the acceptor is less than 8 nm [28]. The following equation can be used to calculate the efficiency (E) of energy transfer between the donor and acceptor [29]:

$$E = 1 - \frac{F}{F_0} = \frac{R_0^6}{R_0^6 + r^6} \quad (6)$$

where r is the distance between the donor and acceptor and R_0 is the critical distance when the transfer efficiency is 50%, which can be calculated by the following equation [30]:

$$R_0^6 = 8.79 \times 10^{-25} K^2 n^{-4} \phi J \quad (7)$$

where K^2 is the orientation factor related to the geometry of the donor–acceptor dipole, n is the refractive index of medium, Φ is the fluorescence quantum yield of the donor, and J expresses the degree of spectral overlap between the donor emission and the acceptor absorption, which could be calculated by the following equation [30]:

$$J = \frac{\int_0^\infty F(\lambda)\varepsilon(\lambda)\lambda^4 d\lambda}{\int_0^\infty F(\lambda) d\lambda} \quad (8)$$

where $F(\lambda)$ is the fluorescence intensity of the donor at wavelength range λ and $\varepsilon(\lambda)$ is the molar absorption coefficient of the acceptor at wavelength λ. In this article, the donor and acceptor were BHb and OTC, respectively. The overlap of the absorption spectrum of OTC and the fluorescence emission spectrum of BHb is shown in Fig. 4. J can be evaluated by integrating the spectra in Fig. 4 according to Eq. (8). In the present case, $K^2 = 2/3$, $n = 1.36$, and $\Phi = 0.062$ [31], According to Eqs. (6)–(8), the following parameters are obtained: $J = 1.3765 \times 10^{-14}$ cm^3 L mol^{-1}, $R_0 = 2.295$ nm, $E = 0.04545$ and $r = 2.37$ nm. The donor to acceptor distance r, which is the average distance from the ligand OTC to the tryptophan residues of the BHb, was less than 8 nm, indicating that the energy transfer from BHb to OTC occurred with high possibility [32]. The results were in accordance with conditions of Förster theory of nonradioactive energy transfer and indicated again a static quenching between OTC and BHb because of the formation of BHb–OTC complex.

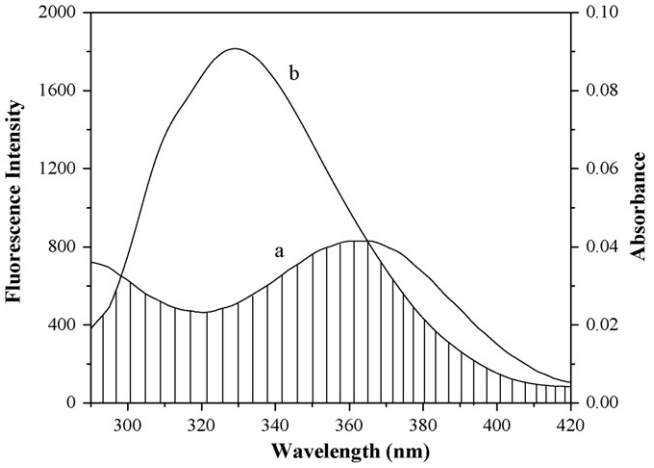

Fig. 4. Overlap of the absorption spectra of OTC (a) with fluorescence emission of BHb (b) (corrected). Conditions: c(OTC) = c(BHb) = 3×10^{-6} mol L^{-1}.

3.5. Investigation on BHb conformation changes

To explore the effect of OTC on the conformation changes of BHb, UV–vis absorption spectra, circular dichroism and synchronous fluorescence measurements were performed.

3.5.1. UV–vis absorption spectra studies

UV–vis absorption spectroscopy technique can be used to explore the structural changes of protein and to investigate protein–ligand complex formation. The UV–vis absorption spectra of BHb in absence and presence of OTC are shown in Fig. 5. It can be seen that BHb has three absorption peaks. The strong absorption peak at 210 nm reflects the framework conformation of the protein [33]. The weak absorption peak at 276 nm appears due to the aromatic amino acids (Trp, Tyr and Phe) [34]. The peak at 405 nm corresponds to the porphyrin-Soret band of BHb [35]. With gradual addition of OTC to BHb solution, the intensity of the peak at 210 nm decreases with red shift and the intensity of the peak at 276 nm increases. The results indicate that the interaction between OTC and BHb leads to the loosening and unfolding of the protein skele-

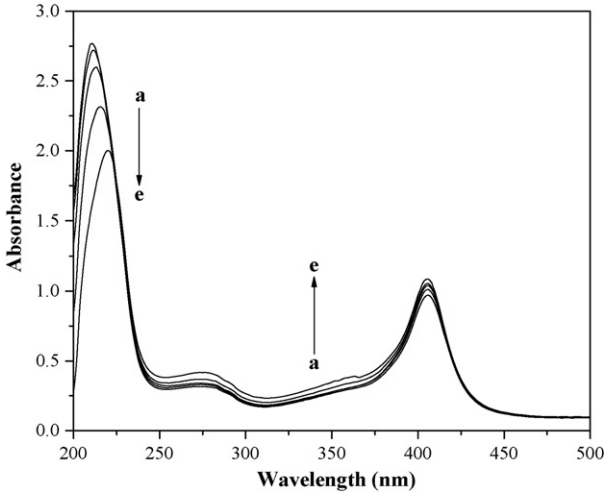

Fig. 5. UV–vis spectra of BHb in presence of different concentrations of OTC (vs. the same concentration of OTC solution). Conditions: BHb: 3×10^{-6} mol L^{-1}; OTC/(10^{-5} mol L^{-1}): (a) 0, (b) 2, (c) 5, (d) 10 and (e) 15; pH 7.4 and $T = 301$ K.

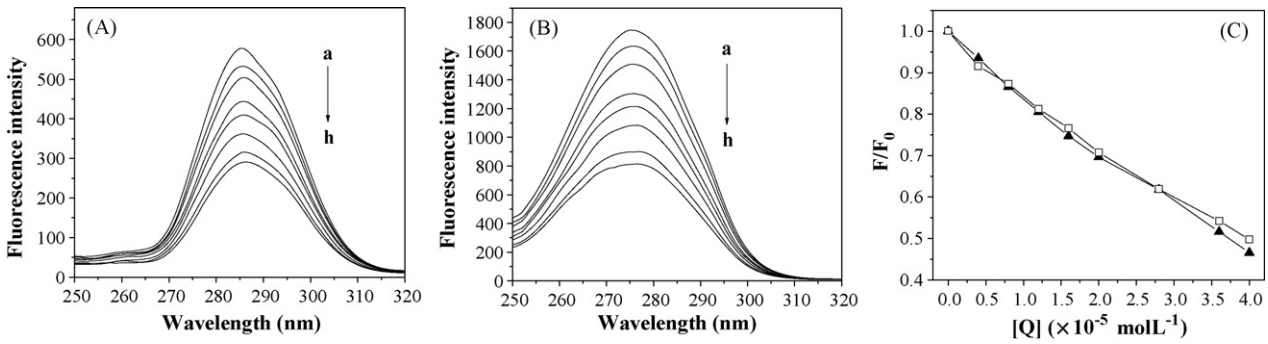

Fig. 6. Synchronous fluorescence spectra of BHb (corrected): (A) $\Delta\lambda = 15$ nm; (B) $\Delta\lambda = 60$ nm; (C) the quenching of BHb synchronous fluorescence by OTC. Conditions: BHb: 3×10^{-6} mol L^{-1}; OTC: (a) 0, (b) 0.4, (c) 0.8, (d) 1.6, (e) 2, (f) 2.8, (g) 3.6 and (h) 4; pH 7.4 and $T = 301$ K; (□) $\Delta\lambda = 15$ nm and (▲) $\Delta\lambda = 60$ nm.

ton and decrease the hydrophobicity of the microenvironment of the aromatic amino acid residues [36]. With increasing OTC concentration, the intensity of the peak at 405 nm increases with no shift, suggesting that OTC can also affect the structure of the heme group, but there is no direct interaction between OTC and the heme groups of BHb [37].

3.5.2. Synchronous fluorescence

The synchronous fluorescence spectroscopy can give information about the molecular environment in the vicinity of the chromospheres. When the wavelength intervals ($\Delta\lambda$) were stabilized at 15 and 60 nm, the synchronous fluorescence gives the characteristic information of tyrosine residues and tryptophan residues, respectively [22].

The synchronous fluorescence spectra of BHb with various amounts of OTC are shown in Fig. 6. It can be seen in Fig. 6(A) that the emission maximum of tyrosine residues is red shifted from 285.4 to 286.4 nm which indicates that the hydrophobicity of the tyrosine residues decreased and tyrosine residues buried in nonpolar hydrophobic cavities were moved to a more hydrophilic environment [38]. In Fig. 6(B), the emission peaks show no shift over the investigated concentration range, which indicates that OTC has no effect on the microenvironment of tryptophan residues in BHb.

BHb contains three Trp and five Tyr residues in each αβ dimmer [20]. The Trp and Tyr residues are symmetric with the BHb cavity as the symmetry center. In Fig. 6(C), it has been shown that the slope was similar when $\Delta\lambda$ was 15 nm or 60 nm, indicating that the opportunity of OTC approaching the Trp and Tyr residues is equal. So, it can be concluded that OTC bind into hemoglobin central cavity to form OTC–BHb complex [24].

3.5.3. Circular dichroism

To ascertain the possible influence of OTC binding on the secondary structure of BHb, CD measurement was performed in the presence of different OTC concentrations (Fig. 7). CD spectra of BHb exhibited two negative bands in the ultraviolet region at about 208 and 222 nm, which was characteristic of α-helix of proteins [39]. The α-helical content of BHb in the absence and presence of OTC were calculated from Eq. (9) to Eq. (10):

$$\mathrm{MRE} = \frac{\text{Observed CD (mdeg)}}{C_p n l \times 10} \tag{9}$$

where C_P is the molar concentration of the protein, n is the number of amino acid residues (574) and l is the path length of the cell (1 cm):

$$\alpha\text{-Helix}(\%) = \frac{-\mathrm{MRE}_{208} - 4000}{33,000 - 4000} \times 100 \tag{10}$$

where MRE_{208} is the observed MRE value at 208 nm, 4000 is the MRE of the β-form and random coil conformation cross at 208 nm, and 33,000 is the MRE value of a pure α-helix at 208 nm. With the addition of OTC to BHb, the α-helicity decreased from 31.06% in free BHb to 29.04% and 26.56% with increasing OTC concentration. The decrease of α-helix content indicates that OTC combines with the amino acid residues of the main polypeptide chain of the protein and destroys their hydrogen bond networks [39,40]. The binding of OTC to BHb induces some conformational changes in BHb which may affect BHb functions [41].

As mentioned above, OTC can bind into hemoglobin central cavity to form OTC–BHb complex, leading to the loosening and unfolding of the protein skeleton, decreasing the hydrophobicity of the microenvironment of tyrosine residues and changing of the structure of the heme group. The α-helix content of BHb decreased due to the binding OTC.

3.6. Computational modeling of the OTC–BHb complex

The crystal structure of BHb taken from the Protein Data Bank (PDB code 1G09) was used to find the binding site of OTC. The best energy ranked result is shown in Fig. 8. It can be seen from Fig. 8(A) and (B) that OTC binds into hemoglobin central cavity which is in accordance with the conclusion of synchronous fluorescence experiment. Fig. 9 shows the binding mode of OTC with the residues of BHb. In OTC, the hydrogen atoms at N 22, O 31 and O 33 are within hydrogen bonding distance from Glu 131, Asp 99 and Glu 101, respectively. The van der Waals interactions exist between OTC and Asp 99, Glu 101, Glu 131 and Lys 104. In addition, the

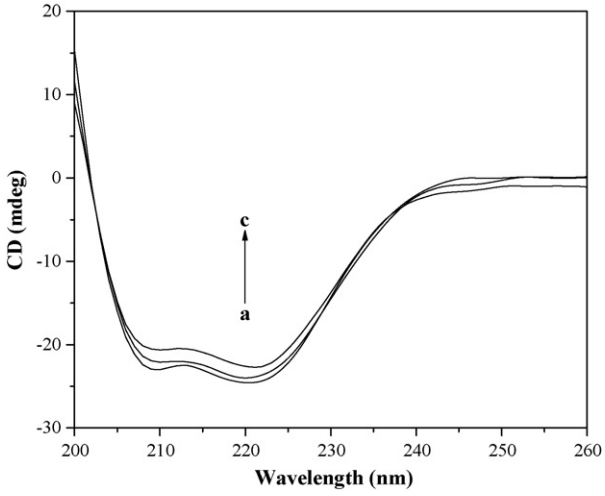

Fig. 7. CD spectra of BHb and BHb–OTC systems. Conditions: BHb: 3.0×10^{-7} mol L^{-1}; OTC: (a) 0, (b) 6×10^{-6} mol L^{-1} and (c) 1.5×10^{-5} mol L^{-1}; pH 7.4 and $T = 301$ K.

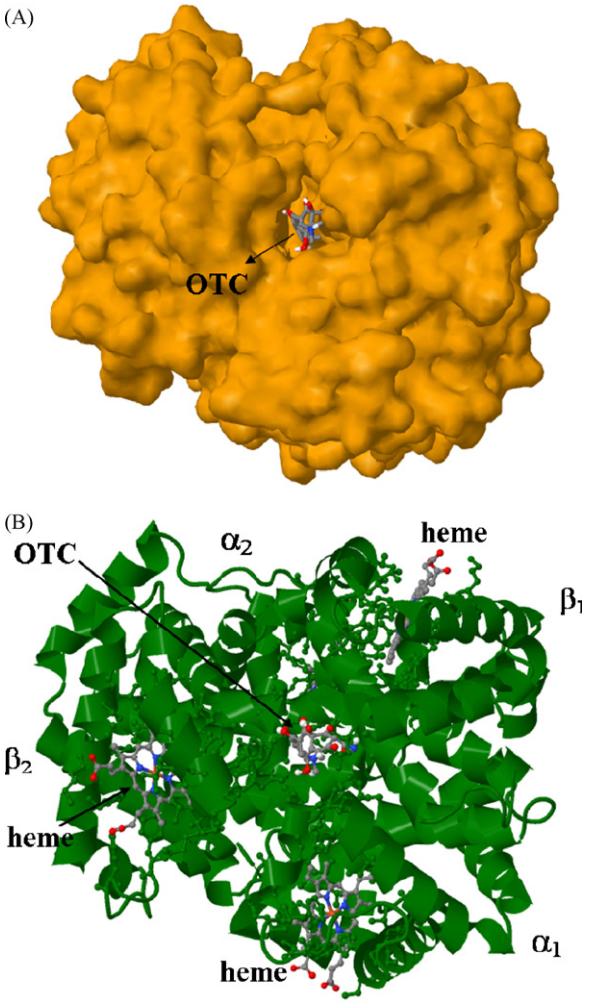

Fig. 8. The binding mode between OTC and BHb. (A) BHb was displayed in surface mode. (B) BHb was displayed in cartoons. The atoms of OTC are colour coded as follows: O, red; N: blue; C, gray; H, white. (For interpretation of the references to color in this figure caption, the reader is referred to the web version of the article.)

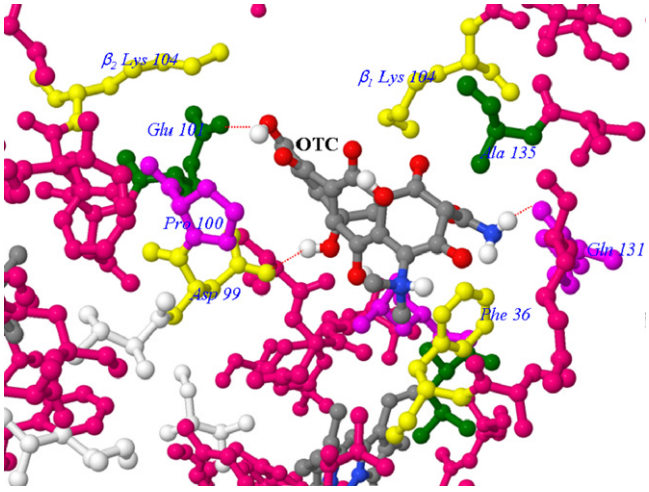

Fig. 9. The enlarged binding mode between OTC and BHb. The atoms of OTC are colour coded as follows: O, red; N: blue; C, gray; H, white. Hydrogen bonds are depicted as red dashed lines. (For interpretation of the references to color in this figure caption, the reader is referred to the web version of the article.)

hydrophobic interaction and some other forces also exist between OTC and BHb, but were not dominating.

4. Conclusions

In this study, the interaction of OTC with BHb was investigated by spectroscopic methods and molecular docking under physiological conditions. OTC can bind into hemoglobin central cavity to form OTC–BHb complex with one binding site and the binding process is spontaneous in which van der Waals and hydrogen bond interactions play a major role. The UV–vis absorption, synchronous fluorescence and CD spectra reveal that the conformational and microenvironment changes of BHb are induced by the binding OTC, which may affect physiological functions of hemoglobin. The work supply valuable information for clarifying the molecular toxic mechanism of OTC in vivo.

Acknowledgements

The work is supported by NSFC (20875055), the Cultivation Fund of the Key Scientific and Technical Innovation Project, Ministry of Education of China (708058) and Excellent Young Scientists and Key Science-Technology Project in Shandong Province (2007BS08005, 2008GG10006012) are also acknowledged.

References

[1] B. Shao, D. Chen, J. Zhang, Y. Wu, C. Sun, Determination of 76 pharmaceutical drugs by liquid chromatography–tandem mass spectrometry in slaughterhouse wastewater, J. Chromatogr. A 1216 (2009) 8312–8318.
[2] M.O. Uslu, I.A. Balcioglu, Comparison of the ozonation and Fenton process performances for the treatment of antibiotic containing manure, Sci. Total Environ. 407 (2009) 3450–3458.
[3] S. Boleas, C. Alonso, J. Pro, C. Fernandez, G. Carbonell, J.V. Tarazona, Toxicity of the antimicrobial oxytetracycline to soil organisms in a multi-species-soil system (MS.3) and influence of manure co-addition, J. Hazard. Mater. 122 (2005) 233–241.
[4] C.S. Ferreira, B.A. Nunes, J.M. Henriques-Almeida, L. Guilhermino, Acute toxicity of oxytetracycline and florfenicol to the microalgae *Tetraselmis chuii* and to the crustacean Artemia parthenogenetica, Ecotoxicol. Environ. Safe. 67 (2007) 452–458.
[5] C. Blasco, A. Di Corcia, Y. Pico, Determination of tetracyclines in multispecie animal tissues by pressurized liquid extraction and liquid chromatography–tandem mass spectrometry, Food Chem. 116 (2009) 1005–1012.
[6] M.C.V. Mamani, F.G.R. Reyes, S. Rath, Multiresidue determination of tetracyclines, sulphonamides and chloramphenicol in bovine milk using HPLC-DAD, Food Chem. 117 (2009) 545–552.
[7] Z. Ye, H.S. Weinberg, M.T. Meyer, Trace analysis of trimethoprim and sulfonamide, macrolide, quinolone, and tetracycline antibiotics in chlorinated drinking water using liquid chromatography electrospray tandem mass spectrometry, Anal. Chem. 79 (2007) 1135–1144.
[8] T. Lunden, S. Miettinen, L.G. Lonnstrom, E.M. Lilius, G. Bylund, Influence of oxytetracycline and oxolinic acid on the immune response of rainbow trout (*Oncorhynchus mykiss*), Fish Shellfish Immunol. 8 (1998) 217–230.
[9] M.M. Qu, L.W. Sun, J. Chen, Y.Q. Li, Y.G. Chen, Z.M. Kong, Toxicological characters of arsanilic acid and oxytetracycline, J. Agro-Environ. Sci. 23 (2004) 240–242.
[10] H.R. De Jonge, Toxicity of tetracyclines in rat-small-intestinal epithelium and liver, Biochem. Pharmacol. 22 (1973) 2659–2677.
[11] E. Omoregie, S.M. Oyebanji, Oxytetracycline-induced blood disorder in juvenile Nile tilapia *Oreochromis niloticus* (Trewavas), J. World Aquacult. Soc. 33 (2002) 377–382.
[12] Y.Q. Wang, H.M. Zhang, Q.H. Zhou, H.L. Xu, A study of the binding of colloidal Fe_3O_4 with bovine hemoglobin using optical spectroscopy, Colloids Surf. A: Physicochem. Eng. Aspects 337 (2009) 102–108.
[13] M.L. Kornguth, C.M. Kunin, Binding of antibiotics to the human intracellular erythrocyte proteins hemoglobin and carbonic anhydase, J. Infect. Dis. 133 (1976) 185–193.
[14] T.C. Mueser, P.H. Rogers, A. Arnone, Interface sliding as illustrated by the multiple quaternary structures of liganded hemoglobin, Biochemistry 39 (2000) 15353–15364.
[15] G. Xiang, C. Tong, H. Lin, Nitroaniline isomers interaction with bovine serum albumin and toxicological implications, J. Fluoresc. 17 (2007) 512–521.
[16] T.A. Halgren, Merck molecular force field. I. Basis, form, scope, parametrization, and performance of MMFF94, J. Comput. Chem. 17 (1998) 490–519.
[17] J.J.P. Stewart, MOPAC2009, Stewart Computational Chemistry, 2009, http://openmopac.net/.

[18] G.M. Morris, R.S. Halliday, R. Huey, W.E. Hart, R.K. Belew, A.J. Olson, D.S. Goodsell, Automated docking using a Lamarckian genetic algorithm and an empirical binding free energy function, J. Comput. Chem. 19 (1998) 1639–1662.
[19] F.J. Solis, R.J.B. Wets, Minimization by random search techniques, Math. Oper. Res. 6 (1981) 19–30.
[20] G. Mandal, S. Bhattacharya, T. Ganguly, Investigations to reveal the nature of interactions between bovine hemoglobin and semiconductor zinc oxide nanoparticles by using various optical techniques, Chem. Phys. Lett. 478 (2009) 271–276.
[21] B. Alpert, D.M. Jameson, G. Weber, Tryptophan emission from human hemoglobin and its isolated subunits, Photochem. Photobiol. 31 (1980) 1–4.
[22] Y.Q. Wang, H.M. Zhang, G.C. Zhang, S.X. Liu, Q.H. Zhou, Z.H. Fei, Z.T. Liu, Studies of the interaction between paraquat and bovine hemoglobin, Int. J. Biol. Macromol. 41 (2007) 243–250.
[23] J. Zhou, X. Wu, X. Gu, L. Zhou, K. Song, S. Wei, Y. Feng, J. Shen, Spectroscopic studies on the interaction of hypocrellin A and hemoglobin, Spectrochim. Acta A: Mol. Biomol. Spectrosc. 72 (2009) 151–155.
[24] Y.Q. Wang, H.M. Zhang, Q.H. Zhou, Studies on the interaction of caffeine with bovine hemoglobin, Eur. J. Med. Chem. 44 (2009) 2100–2105.
[25] G. Paramaguru, A. Kathiravan, S. Selvaraj, P. Venuvanalingam, R. Renganathan, Interaction of anthraquinone dyes with lysozyme: evidences from spectroscopic and docking studies, J. Hazard. Mater. 175 (2010) 985–991.
[26] H.M. Zhang, Y.Q. Wang, Q.H. Zhou, G.L. Wang, Molecular interaction between phosphomolybdate acid and bovine hemoglobin, J. Mol. Struct. 921 (2009) 156–162.
[27] T. Förster, O. Sinanoglu (Eds.), Modern Quantum Chemistry [M], Academic Press, New York, 1996.
[28] B. Valeur, J.C. Brochon, New Trends in Fluorescence Spectroscopy, Springer Press, Berlin, 2001.
[29] W.D. Horrocks Jr., A.P. Snyder, Measurement of distance between fluorescent amino acid residues and metal ion binding sites. Quantitation of energy transfer between tryptophan and terbium (III) or europium (III) in thermolysin, Biochem. Biophys. Res. Commun. 100 (1981) 111–117.
[30] Y.Z. Zhang, X.X. Chen, J. Dai, X.P. Zhang, Y.X. Liu, Y. Liu, Spectroscopic studies on the interaction of lanthanum(III) 2-oxo-propionic acid salicyloyl hydrazone complex with bovine serum albumin, Luminescence 23 (2008) 150–156.
[31] A. Haouz, S. El Mohsni, C. Zentz, F. Merola, B. Alpert, Heterogeneous motions within human apohemoglobin, Eur. J. Biochem. 264 (1999) 250–257.
[32] Y.Z. Zhang, B. Zhou, X.P. Zhang, P. Huang, C.H. Li, Y. Liu, Interaction of malachite green with bovine serum albumin: determination of the binding mechanism and binding site by spectroscopic methods, J. Hazard. Mater. 163 (2009) 1345–1352.
[33] Q. Yang, J. Liang, H. Han, Probing the interaction of magnetic iron oxide nanoparticles with bovine serum albumin by spectroscopic techniques, J. Phys. Chem. B 113 (2009) 10454–10458.
[34] S. Patil, A. Sandberg, E. Heckert, W. Self, S. Seal, Protein adsorption and cellular uptake of cerium oxide nanoparticles as a function of zeta potential, Biomaterials 28 (2007) 4600–4607.
[35] X. Bao, Z. Zhu, N.Q. Li, J. Chen, Electrochemical studies of rutin interacting with hemoglobin and determination of hemoglobin, Talanta 54 (2001) 591–596.
[36] T. Wu, Q. Wu, S. Guan, H. Su, Z. Cai, Binding of the environmental pollutant naphthol to bovine serum albumin, Biomacromolecules 8 (2007) 1899–1906.
[37] Q.H. Zhou, Y.Q. Wang, H.M. Zhang, G.C. Zhang, Z.H. Fei, Z.T. Liu, Spectroscopic studies on the Interaction between imidacloprid and bovine hemoglobin (BHb), J. Instrum. Anal. 26 (2007) 368–372.
[38] B. Klajnert, M. Bryszewska, Fluorescence studies on PAMAM dendrimers interactions with bovine serum albumin, Bioelectrochemistry 55 (2002) 33–35.
[39] J.Q. Lu, F. Jin, T.Q. Sun, X.W. Zhou, Multi-spectroscopic study on interaction of bovine serum albumin with lomefloxacin–copper(II) complex, Int. J. Biol. Macromol. 40 (2007) 299–304.
[40] X.C. Shen, X.Y. Liou, L.P. Ye, H. Liang, Z.Y. Wang, Spectroscopic studies on the interaction between human hemoglobin and US quantum dots, J. Colloid Interface Sci. 311 (2007) 400–406.
[41] E.P. Melo, M.R. Aires-Barros, S.M. Costa, J.M. Cabral, Thermal unfolding of proteins at high pH range studied by UV absorbance, J. Biochem. Biophys. Methods 34 (1997) 45–59.